Development of a Transferable Guest−Host Force Field for Adsorption of Hydrocarbons in Zeolites. II. Prediction of Alkenes Adsorption and Alkane/Alkene Selectivity in Silicalite

Pierre Pascual,[†,‡] Philippe Ungerer,[†,‡] Bernard Tavitian,[‡] and Anne Boutin*[,†]

Laboratoire de Chimie Physique, bâtiment 349, Université Paris-Sud, CNRS, 91405 Orsay Cedex, France and Institut Français du Pétrole, 92852, Rueil-Malmaison, France

Received: June 30, 2003; In Final Form: September 8, 2003

Alkene pure components and alkane/alkene binary mixtures adsorption isotherms are computed by grand canonical Monte Carlo simulations. The anisotropic united atom potential optimized from experimental isotherms of butane in silicalite is used without further adjustement to predict the behavior of alkane and alkene molecules in silicalite. Simulated results are in good agreement with available experimental data. Selectivity of silicalite toward alkane/alkene mixtures is driven by enthalpic effects at low coverage and by entropic effects at saturation. An interesting reversal of ethane/ethene selectivity with temperature is predicted.

1. Introduction

A detailed knowledge of the adsorption−desorption mechanism of hydrocarbons in zeolitic microporous materials is of great scientific interest in the context of petrochemical applications such as separation processes.[1,2] Experiments and molecular simulations can be used simultaneously to understand the separation mechanism of fluid mixtures at the microscopic level and increase industrial process performances.[3,4] The aim of our work is to develop a transferable force field for adsorption of hydrocarbons in zeolites. Few experimental data[5−7] concerning alkene adsorption in silicalite are available whereas separation of mixtures of alkane and alkene molecules is of a great interest in petrochemical industry. In a previous work,[8] we have reinvestigated the adsorption of linear and branched alkanes in silicalite and developed a new hydrocarbon−zeolite semiempirical force field. We present here an extension of this new force field to alkene adsorption as well as binary mixtures of alkane and alkene molecules adsorption.

The simple idea developed in the first part of the work[8] was to compute some zeolite potential parameters (in silicalite the Lennard-Jones parameters of oxygen: σ_o and ϵ_o) through an adjustment of simulation results to experimental data. To start with, a neutral (i.e., noncationic) zeolite was selected for which the oxygen parameters were the only ones to be adjusted. These parameters can then be combined with adsorbate−adsorbate anisotropic united atom (AUA-4) parameters[9,10] to yield adsorbent−adsorbate parameters without any further adjustment. The Lorentz−Berthelot combining rules are used to obtain cross potential parameters from the individual molecular group values. We have chosen to use the experimental adsorption isotherm of butane to adjust the oxygen parameters.[8] The strategy used here to develop the guest−host force field is somewhat different from the one previously used by Smit and co-workers[11,12] (see ref 8 for details).

We have thus successfully reproduced the adsorption isotherms of linear and branched alkanes (from C1 to C9) in the temperature range 270−374 K.[8] The extension to alkene molecules, for which adsorbate−adsorbate parameters are available,[10] is straightforward and allows a total prediction of the single component and binary mixtures adsorption properties. Up to now, we have limited ourselves to nonelectrostatic interactions. Although alkene molecules can exhibit significant dipole moments, this approximation has been used in the development of the AUA force field for bulk alkene fluids[10] and led to good agreement with experiments. We have thus decided, as a starting point, to neglect the electrostatic interactions in the simulations of alkene adsorption in silicate.

In the next section, the methodology used in this work is described. In section 3 we report and discuss the results obtained for nine pure components (ethene, propene, but-1-ene, (Z)-but-2-ene, (E)-but-2-ene, isobutene, pent-1-ene, hex-1-ene, hept-1-ene) and for four binary mixtures (ethane/ethene, propane/propene, heptane/hept-1-ene, and (Z)-but-2-ene/(E)-but-2-ene) at various temperatures.

2. Models and Simulations

Grand canonical Monte Carlo simulation is used to study adsorption of hydrocarbons in silicalite zeolite. The crystal structure of silicalite-1 zeolite has been taken from X-ray diffraction experiments.[13] The orthorhombic unit cell parameters are $a = 20.07$, $b = 19.92$, and $c = 13.42$ Å. The silicalite framework contains interconnected pore channels of two types: straight channels which run in the direction of the y axis and zigzag channels which run in the direction of the x axis (see Figure 1). Three type of sites can be extrapolated in a unit cell of silicalite, four straight channels (SC), four zigzag channels (ZC), and four intersections (I). The partial volume of each type of sites can be approximated by geometrical considerations to 33, 45, and 22%, respectively, for SC, ZC, and I.[8] The zeolite framework is considered as rigid[14] and the guest−host interactions are calculated on a grid of points prior to simulations. The grid mesh is about 0.2 Å in the three space directions. The simulation box is generally composed of two ($1 \times 1 \times 2$) silicalite unit cells with periodic boundary conditions. When the number of adsorbed molecules is lower than four per unit cell, the simulation box is increased up to eight ($2 \times 2 \times 2$) unit cells to improve statistics. No significant difference has

* Address correspondence to this author.
† Université Paris-Sud.
‡ Institut Français du Pétrole.

10.1021/jp0358634 CCC: $27.50
Published on Web 12/09/2003

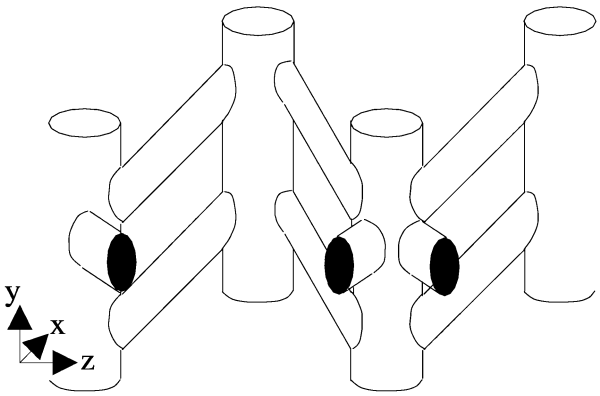

Figure 1. Schematic view of the pore structure of silicalite.

TABLE 1: Intermolecular Guest−Guest Lennard-Jones Parameters of Alkane and Alkene Force Centers in the AUA Model[a]

	σ (Å)	ϵ (K)	δ (Å)
CH (sp3)	3.36	50.98	0.646
CH_2 (sp3)	3.46	86.29	0.384
CH_3 (sp3)	3.61	120.15	0.216
CH_4	3.74	149.92	
C (sp2)	3.02	61.90	
CH (sp2)	3.32	90.60	0.414
CH_2 (sp2)	3.48	111.10	0.295

[a] References 9 and 10.

been observed in simulated adsorption quantities at high loading between the two box sizes.

The anisotropic united atom (AUA) model is used to describe the adsorbate molecules.[15,16] Intramolecular interactions include bond-bending and torsion potentials as well as nonbonded interactions described by a Lennard-Jones 6−12 potential. More details on intramolecular potential parameter values are given in previous works.[8−10] Guest−guest intermolecular interactions are calculated by a 6−12 Lennard-Jones potential with a cutoff distance fixed at 9.96 Å. Lennard-Jones parameters of hydrocarbons (see Table 1) are taken from Ungerer et al.[9] for alkanes and from Bourasseau et al.[10] for alkenes.

The guest−host potential is of the "Kiselev type".[4,14] It contains a single effective LJ term which acts between the oxygen atoms of the framework and each of the anisotropic united atoms of the guest molecules. The zeolite oxygen atom parameters are $\sigma_o = 3.00$ Å and $\epsilon_o = 93.53$ K. The hydrocarbons/hydrocarbons and hydrocarbons/zeolite interaction parameters are determined from Lorentz−Berthelot combining rules (eq 1) and are used to evaluate interactions between any centers of force.

$$\epsilon_{ij} = \sqrt{\epsilon_{ii}\epsilon_{jj}}$$
$$\sigma_{ij} = \frac{\sigma_{ii} + \sigma_{jj}}{2} \qquad (1)$$

Only butane (i.e., CH_2 and CH_3 force centers) was used in the oxygen atom optimization process. Simulation results obtained with molecules which include at least another force center are thus pure predictions.

Adsorption isotherms are computed using biased grand canonical ensemble (μ,V,T) simulations.[17] Translation, rotation, regrowth,[17] flip,[18] reptation,[19] and insertion-destruction moves allow a good sampling of potential energy hypersurface. However, the CBMC move has to be modified to deal with AUA model[20] and the reptation move is not suitable for alkene

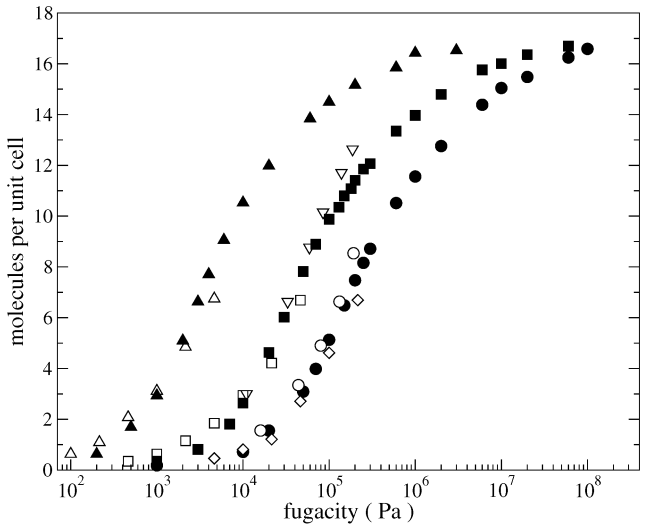

Figure 2. Simulated ethene adsorption isotherms in silicalite carried out at 250, 306, and 350 K (from left to right, filled symbols). Experiments of Choudary et al.[5,6] performed at 306 (▽) and 353 K (○) and those of Stach et al.[7] carried out at 250 (△), 300 (□), and 350 K (◇) are reported.

simulation because of the presence of a double bond. Simulations were performed during at least five million steps to reach convergence and are extended a further million steps when better statistics is required. The chemical potential of each compound is calculated from the partial fugacity $y_i P_i$ of the vapor phase by using the ideal gas relation (eq 2).

$$\frac{\mu_i}{k} = T \ln\left(\frac{y_i P_i}{P_o}\right) \qquad (2)$$

where P_o is the pressure of the reference state.

We have checked that the approximation of ideal gas is satisfactory for alkanes and alkenes below 1 MPa under thermodynamics conditions used in this study by separately simulating gas-phase properties.

Simulation results yield total adsorption but experiments measure excess adsorption, as emphasized by Talu and Myers.[30] We have checked in our case that the difference between total and excess quantities is always lower than 0.1 molecule per unit cell.

The heat of adsorption at zero coverage Q_{st}^0 is calculated from a fluctuations method.[8,21] The single site (SSL) and dual site (DSL) Langmuir models[22] are used to fit simulated isotherms, which allows to determine "effective site" adsorption enthalpies and entropies averaged over loading and temperature. A bayesian approach is used to ascertain the identification of the set of fitting parameters.[8] The final uncertainties on the enthalpies and entropies are estimated to be 1 kJ mol^{-1} and 2 J mol^{-1} K^{-1}, respectively.

3. Results and Discussion

3.1. Single Adsorption Isotherms. Computed adsorption isotherms of ethene C_2H_4 carried out at 250, 306, and 350 K have been compared with available experimental data[5−7] (see Figure 2). Simulated isotherms are in a good agreement with experiments. Available experimental points are concentrated at the beginning of the isotherms where the slope is high and the agreement between experiments and simulations is difficult to achieve as observed in most of the previous simulation works. The saturation plateau is reached for 16 molecules per unit cell,

TABLE 2: Enthalpies and Entropies of Adsorption of Alkanes and Alkenes in Silicalite as Obtained from the Langmuir Model[a]

	$-\Delta H_{ads}^{o}$ (1) (kJ mol^{-1})	$-\Delta S_{ads}^{o}$ (1) (J mol^{-1} K^{-1})	$-\Delta H_{ads}^{o}$ (2) (kJ mol^{-1})	$-\Delta S_{ads}^{o}$ (2) (J mol^{-1} K^{-1})	Q_{st}^{o} (kJ mol^{-1})
ethane	30.8	181	30		
ethene	26.6	175	27		
propane	38.9	189	39		
propene	39.2	193	38		
heptane	75.6	220	78.9	287	75
heptene	74.3	221	72.0	268	73

[a] The labels (1) and (2) refer to the first and second adsorption site in the case of a DSL fit. Q_{st}^{o} is the isosteric heat of adsorption at zero coverage obtained by the fluctuations method at 300 K.

TABLE 3: Probability (%) To Find Alkene Molecule Center of Mass (cm) in a Straight Channel (SC), in a Zigzag Channel (ZC), or in an Intersection (I) of Silicalite at 300 K[a]

		low coverage				saturation			
		⟨N⟩	SC	ZC	I	⟨N⟩	SC	ZC	I
ethene	cm	0.8	31	47	22	16.0	25	49	26
propene	cm	0.6	28	43	29	11.9	33	36	31
but-1-ene	cm	0.9	23	39	37	9.9	25	49	26
	head		*24*	*40*	*36*		*20*	*45*	*36*
(Z)-but-2-ene	cm	1.1	17	28	55	9.9	30	40	30
	head		*16*	*35*	*49*		*28*	*42*	*30*
(E)-but-2-ene	cm	0.6	17	26	57	9.1	32	41	27
	head		*17*	*33*	*50*		*27*	*43*	*30*
isobutene	cm	1.0	6	16	79	9.9	22	39	39
	head		*12*	*26*	*62*		*27*	*41*	*32*
pent-1-ene	cm	0.6	19	38	43	9.0	43	44	13
	head		*20*	*43*	*37*		*5*	*47*	*48*
hex-1-ene	cm	0.6	18	32	50	8.0	42	50	8
	head		*26*	*34*	*40*		*14*	*50*	*36*
hept-1-ene	cm	0.7	19	28	53	7.0	8	56	36
	head		*34*	*29*	*37*		*34*	*49*	*17*

[a] The same probability for chain heads is indicated in italic.

that is, the same loading as for ethane in silicalite. Ethane and ethene locations during adsorption process are very similar. In both cases, the adsorption sites are identical and two molecules can simultaneously fill the same zigzag channel at high pressure (see Table 3). At very low coverage (0.8 molecule per unit cell), ethene molecules equally fill all available pore space. The partial occupancies (31, 47, and 22%) of the three types of channels correspond to the volume fraction. At saturation, the specific ordering observed for ethane is less pronounced for ethene molecules. This is not suprising because the molecular length is shorter with ethene than with ethane and is not commensurate with zeolite structure. The first part of adsorption isotherms, when all sites can be considered as equivalent and only occupied by a single molecule, allows the determination of enthalpy and entropy of adsorption by fitting this region with single site langmuir (SSL) model (see Table 2).

The adsorption isotherms of alpha olefins from ethene to hept-1-ene have been calculated at 300 K (see Figure 3). Simulated values are in a good agreement with available experimental data.[7] A comparative study with alkanes reveals strong similarities: the adsorbed quantity at saturation decreases with carbon number and are identical for alkane and alkene with the same carbon number.[8]

For propene, a detailed study has been done to determine the enthalpy and the entropy of adsorption. The isotherms at 300, 330, and 360 K have been used to evaluate Langmuir parameters from a bayesian approach[8] (see Table 2). Each silicalite channel can accept one propene molecule only. This leads to 12 equivalent adsorption sites that are totally filled at

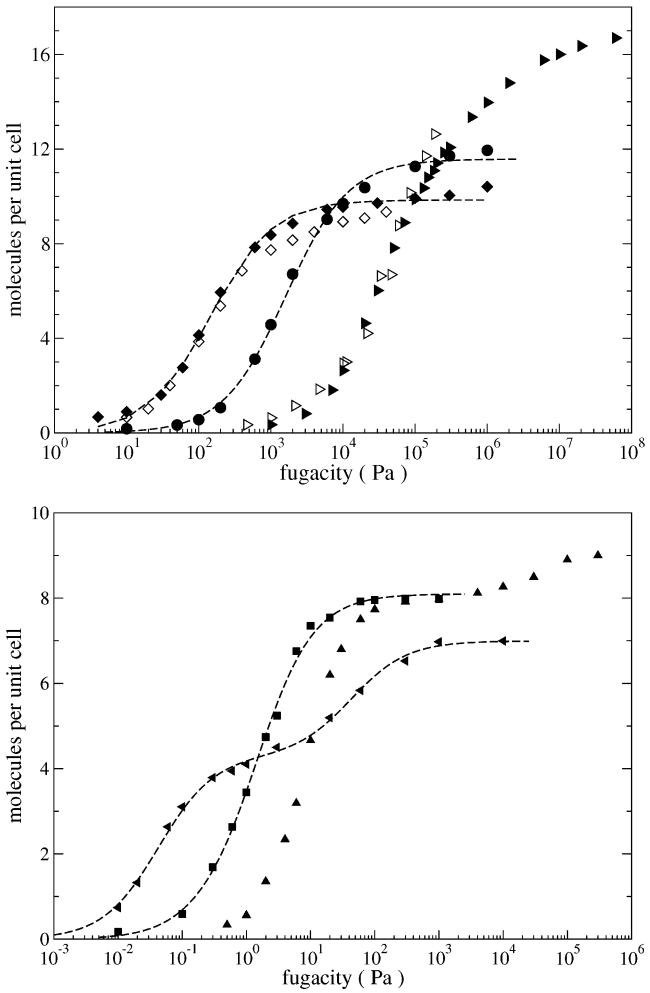

Figure 3. Alpha olefins simulated adsorption isotherms in silicalite at 300 K (ethene (rightward solid triangle), propene (●), but-1-ene (◆), pent-1-ene (▲), hex-1-ene (■), hept-1-ene (leftward solid triangle)). Available experiments[5−7] (open symbols) and Langmuir fits (dotted lines) are indicated.

saturation. At low coverage, a weak preference for the zigzag channels (43% of adsorbed molecules) is observed.

For but-1-ene, the saturation plateau is reached for 10 molecules per unit cell because half of the intersections are unoccupied. This may be attributed to the blocking of half of these sites by molecules located in straight channels. This mechanism is exactly the same as for the *n*-butane molecules in silicalite.[8] At low coverage, all sites are filled with a weak preference for the zigzag channels (39%). At saturation, all zigzag and straight channels are filled and two intersections are thus blocked.

Pent-1-ene is the shortest molecule for which both Langmuir models fail. This is because the molecular length of pentene is larger than the straight channel length but smaller than the zigzag channel length. Table 3 clearly shows that all the straight channels are filled (43% of centers of mass are located in SC) whereas only 5% of molecule heads are sitting in SC. However, at high pressure, pentene molecules leave some free space in intersection that allows one new insertion. These moves in cavity pores modify the description of adsorption sites and the SSL Langmuir model is no longer suitable. This location mechanism is illustrated by the step observed at high pressure on the adsorption isotherm. At saturation (9.0 molecules per unit cell), all straight and zigzag channels are filled (respectively, 43 and 44%) as well as one intersection (13%).

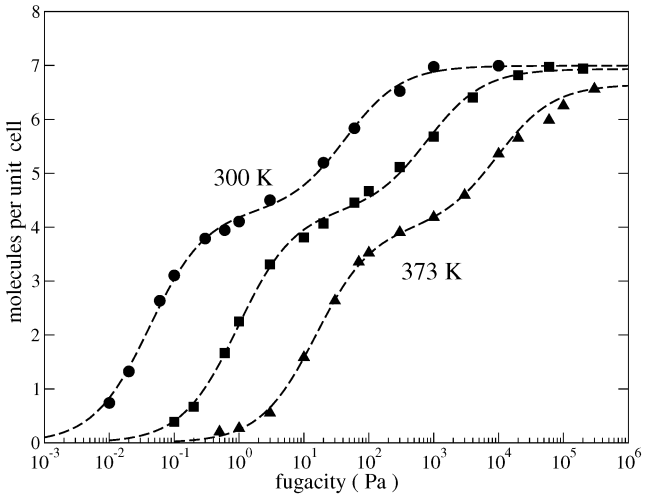

Figure 4. Hept-1-ene simulated adsorption isotherms in silicalite at 300, 333, and 373 K (filled symbols) and Langmuir DSL curves (dotted lines).

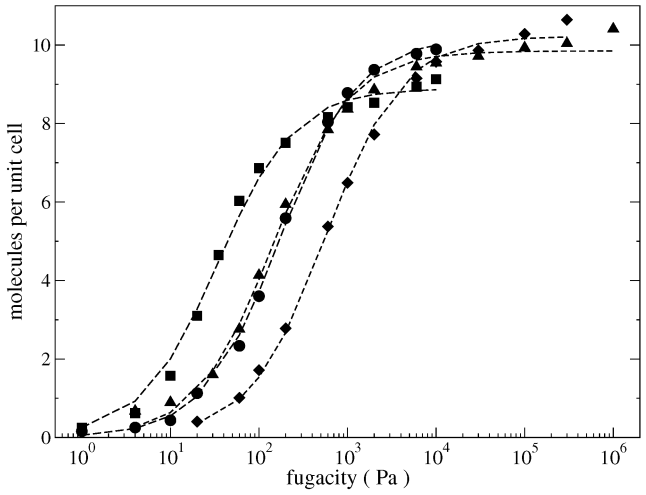

Figure 5. Butene isomers simulated adsorption isotherms in silicalite at 300 K ((Z)-but-2-ene (●), (E)-but-2-ene (■), but-1-ene (▲), isobutene (◆)) and Langmuir DSL curves (dotted lines).

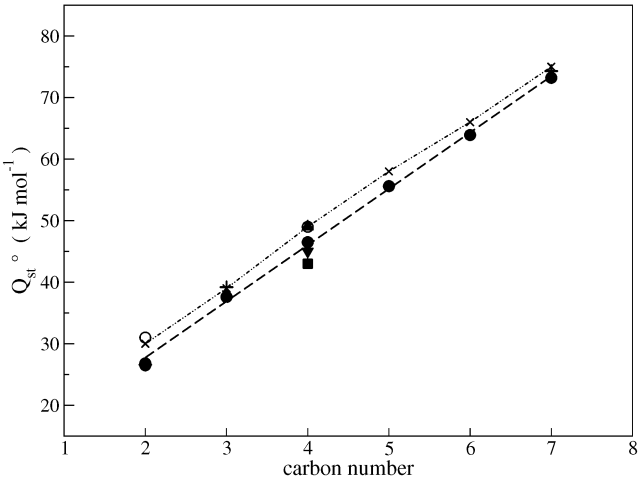

Figure 6. Heat of adsorption of alkenes in silicalite at 300 K calculated by the fluctuations method (alpha olefins (●), isobutene (■), (E)-but-2-ene (▲), (Z)-but-2-ene (▼), experiment[5−7] (○), results obtained by Langmuir theory (+)). Heat of adsorption of linear alkanes (×) are reported.

An inflection point appears for hex-1-ene and a two-step isotherm is observed for hept-1-ene. The geometrical considerations put forward for alkane molecules[12,23−25] turn out to be true for alkene molecules. The hexene molecule can form a structure commensurate with the zigzag channel. The heptene molecule is longer than ZC, so that all the sites are blocked when four heptene molecules are adsorbed in silicalite. The insertion of a fifth molecule requires a rearrangement in channels that explains the first plateau.

Adsorption isotherms of heptene are plotted in Figure 4 at 300, 333, and 373 K. From Langmuir parameters obtained by the bayesian approach, adsorption enthalpies and entropies of both sites are determined and compared with heptane (see Table 2). The first type of sites of alkane and alkene is similar whereas the second type of sites is quite different. At low loadings, the rigid double bond weakly influences the location of the long alkyl chain and the same behavior is observed for heptene and heptane molecules. At high coverage, when the insertion requires a strong reorganization in cavity pores, the double bond seems to play an important role.

A detailed study of butene isomers has been carried out to shed light on the capability of AUA potential to differentiate between molecular isomers behavior. Adsorption isotherms of but-1-ene, (Z)-but-2-ene, (E)-but-2-ene, and isobutene at 300 K have been plotted in Figure 5. The maximum of adsorption is similar for all isomers. The location mechanisms are quite different. The preferential adsorption site is closely linked to the molecular geometries. But-1-ene and *n*-butane molecules have similar geometries and exhibit the same behavior in silicalite. For but-2-ene isomers, the rigid middle double bond increases the radius of gyration of the molecule. Intersection sites are thus filled preferentially at low coverage. At saturation, we find three molecules in straight channels, four in zigzag channels, and three in intersections. For isobutene, at low coverage (1.0 molecules per unit cell), 79% of adsorbed molecules are found to fill intersections. At saturation (9.9 molecules per unit cell), all intersections and zigzag channels are occupied, whereas only two straight channels are filled. This location is exactly the same as in isobutane.[8] Indeed, for such a planar branched alkene, the insertion in intersections is easier than in straight and zigzag channels.

The heat of adsorption calculated from the fluctuations method[8] is plotted as a function of carbon number in Figure 6. Simulated values are in good agreement with available experimental data,[5,6,7] indicating an increase of 9.1 kJ mol^{-1} per CH_2 added on the main chain. Previous works[8,12,24] on alkanes in silicalite have shown an increase in the heat of adsorption amounting to about 9.3 kJ mol^{-1} per CH_2. Moreover, adsorption enthalpies obtained from Langmuir parameters are also consistent with the heats of adsorption calculated by the fluctuations method. The difference between the adsorption heats of alpha-alkenes and alkanes is about 2−3 kJ mol^{-1} whatever the carbon number.

3.2. Binary Mixtures Coadsorption Isotherms. Adsorption selectivity studies have been carried out on alkane/alkene mixtures (see Figures 8−10) and on a mixture of diastereoisomers (see Figure 7). All coadsorption isotherms are plotted as a function of the total fugacity of the mixture. In all cases, the partial fugacity of both compounds in the binary mixture was fixed to the same value. We have checked that this condition leads to equimolar mixtures within less than 3% in the temperature and pressure range used for computing the isotherms.

We have found that, at low pressure, silicalite selectively adsorbs the alkane component in alkane/alkene mixtures of equal carbon number and the (E)-isomer in the but-2-ene diastereo-

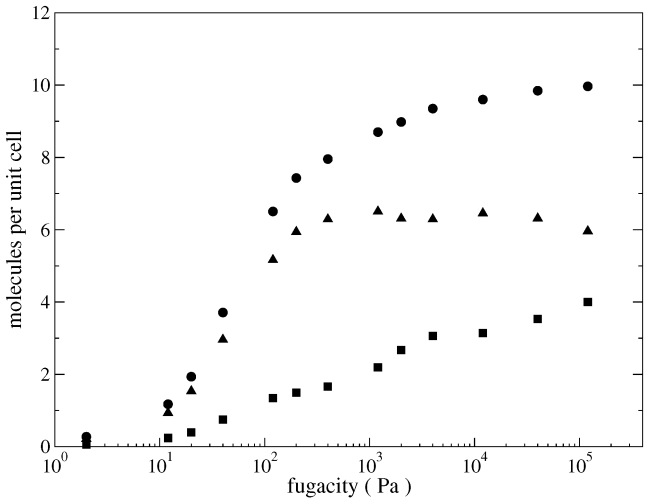

Figure 7. Adsorption isotherm of binary mixture of (Z) and (E)-but-2-ene at 300 K (total adsorbed quantity (●), (Z)-but-2-ene (■), (E)-but-2-ene (▲)), as a function of the total fugacity of the mixtures.

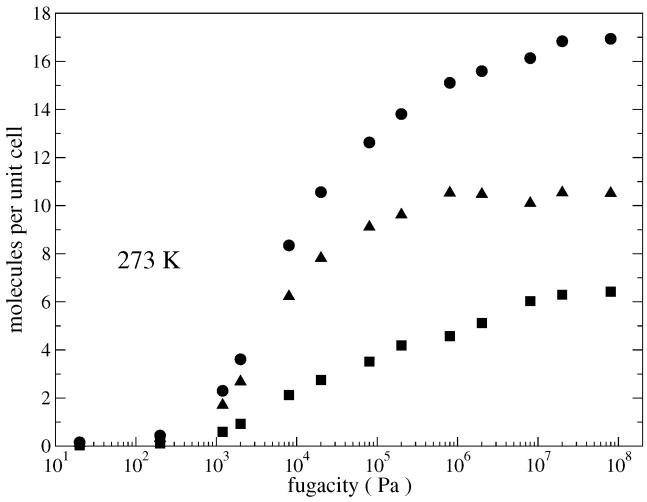

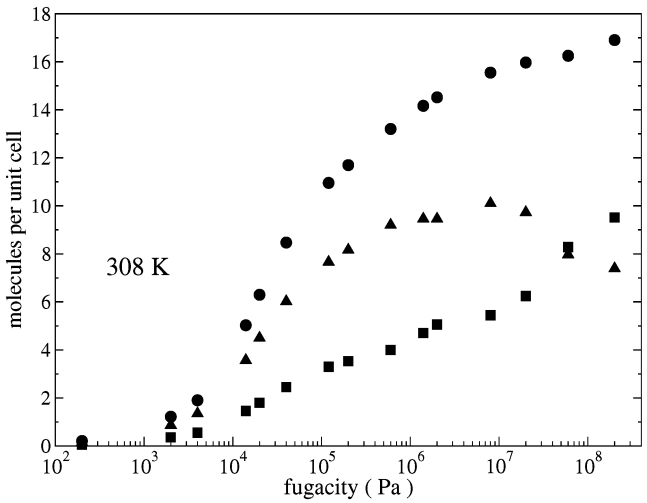

Figure 8. Adsorption isotherm of binary mixture of ethane/ethene at 273 and 308 K (total adsorbed quantity (●), ethene (■), ethane (▲)), as a function of the total fugacity of the mixtures.

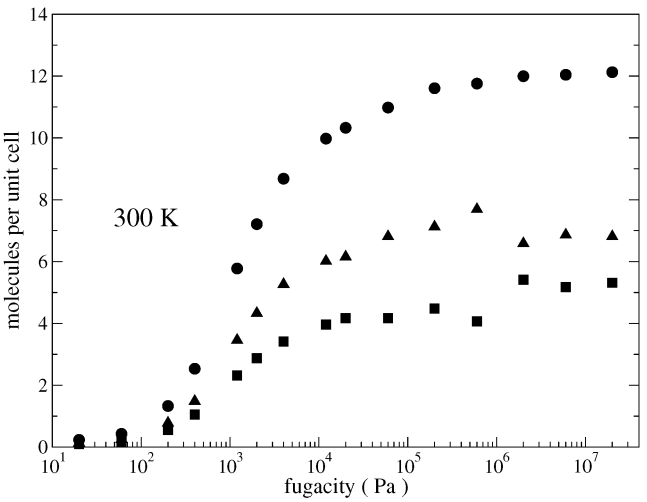

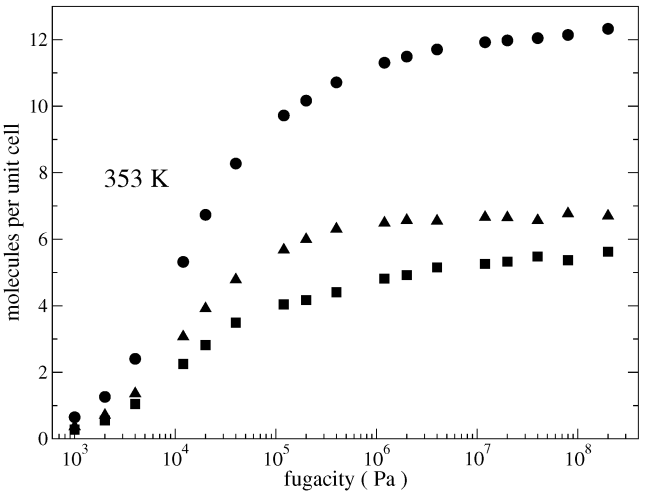

Figure 9. Adsorption isotherm of binary mixture of propane/propene at 300 and 353 K (total adsorbed quantity (●), propene (■), propane (▲)), as a function of the total fugacity of the mixtures.

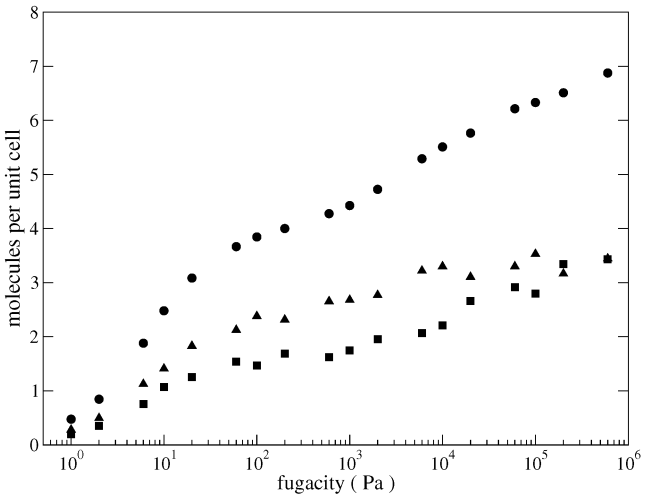

Figure 10. Adsorption isotherm of binary mixture of heptane/heptene at 373 K (total adsorbed quantity (●), heptene (■), heptane (▲)), as a function of the total fugacity of the mixtures.

isomer mixture. The selectivity factor α is simply calculated as the ratio of the number of alkane to alkene molecules since we are dealing with equimolar mixtures. This corresponds to the equilibrium sorption selectivity. As in ref 26, no kinetic term was taken into account here. In all cases, we have found that α decreases with pressure.

In the ethane/ethene mixture at 273 K, the selectivity factor α decreases smoothly from 2.9 at a pressure of 2×10^3 to 1.6 at 8×10^7 Pa. The preferential adsorption of alkane ($\alpha > 1$) is

consistent with the computed adsorption heats of the pure components (see Table 2). However, the adsorption entropy of ethane is larger than that of ethene. One can thus expect that, at sufficiently high temperature, the entropy effect compensates the enthalpy effect. Indeed, at 308 K, we observed a reversal of selectivity at high loadings and silicalite preferentially adsorbs ethene molecules at saturation ($\alpha = 2.3$ at 6×10^5 Pa and 0.8 at saturation).

For propane/propene mixture, a similar trend is observed. However, the difference between adsorption heats of propane and propene is smaller than in the ethane/ethene case. The selectivy factor is thus also smaller ($\alpha = 1.4$, 1.6, and 1.3 at 2×10^2, 6×10^3, and 2×10^8 Pa, respectively, at 300 K). The entropies of adsorption are quite similar (-189 and -193J mol^{-1} K^{-1} for propane and propene, respectively) and the selectivity is not significantly modified with increasing temperature. From a qualitative point of view, the "effect" of a single double bond on the properties of a molecular fluid is smoothed out as the number of carbon atoms increases in the molecule.

For heptane/heptene mixture, the behavior is more complex because of the existence of two distinct adsorption sites. The first adsorption site is quite similar for the two molecules (75.6 and 74.3 kJ mol^{-1} for heptane and heptene, respectively) and this leads to a weak selectivity in favor of heptane at low coverage ($\alpha = 1.4$ at 2 Pa). However, the second adsorption site is quite different. Although enthalpic effects are strongly in favor of heptane (78.9 and 72.0 kJ mol^{-1} for heptane and heptene, respectively), selectivity tends to decrease because of entropic effects. Indeed, the important difference between entropies of adsorption in the second site (-287 and -268 J mol^{-1} K^{-1} for heptane and heptene, respectively) counterbalances the enthalpic effects. No selectivity is observed at saturation ($\alpha = 1$).

For the but-2-ene distereoisomers mixture, a selectivity in favor of the E isomer is observed which decreases with loading. The selectivity factor is 3.9, 3.8, and 1.5 at 12, 4×10^2, and 1.2×10^5 Pa, respectively. The selectivity at low loading is driven by energetic effects. The computed adsorption heats are 50 and 45 kJ mol^{-1} for (E) and (Z)-isomers, respectively. As for alkane/alkene coadsorption, the decrease of the selectivity factor at saturation can be interpreted in terms of entropic effects. We have observed that the (Z)-but-2-ene isomer fits better at intersection sites that the (E)-isomer (see Table 3).

We have shown that the difference between adsorption heats is responsible for the observed selectivity at low coverage and that at high coverage, selectivity is driven by entropic effects. This is consistent with the "configurational entropy effects" described by Krishna et al. for coadsorption of mixtures of branched and linear alkanes in silicalite.[27,28] In alkane/alkene mixtures, the configurational entropy effects favor alkenes because such molecules "pack" more efficiently within silicalite pores. In this work, pure component adsorption data at different temperature enabled us to evaluate the adsorption heat and entropy of pure components. The computed values are perfectly consistent with the observed selectivity in coadsorption simulations. The silicalite zeolite appears to be less selective than the all-silica DD3R.[29] A strong selectivity has been recently measured in this latter zeolite that is interpreted in terms of a shape selectivity. This seems to be due to an exclusion of the propane molecules from the eighth-ring windows.

4. Conclusion

A methodology has been developed to determine a transferable force field for adsorption in zeolites. We use simple combining rules for the determination of cross potential parameters and the anisotropic united atom AUA model for hydrocarbon interactions. We have been able to predict the adsorption isotherms of alkanes, alkenes, and mixtures of alkane and alkene molecules in silicalite zeolite. Our results agree with available experimental data.

This force field may now be extended to aluminosilicate of zeolites. The guest−host potential will contain LJ and Coulombic terms, acting between extraframework cations and the guest molecules. Whether or not this force field will still be transferable from one guest−host system to another is still an open question.

References and Notes

(1) Guisnet, M.; Gilson, J. P. *Zeolites for Cleaner Technologies*; Imperial College Press: London, 2002.
(2) Neuzil, R. W. U.S. Patent 3,558,732, 1971.
(3) Smit, B.; Krishna, R. *Chem. Eng. Sci.* **2003**, *58*, 557.
(4) Fuchs, A. H.; Cheetham, A. K. *J. Phys. Chem. B* **2001**, *105*, 7375.
(5) Choudary, V. R.; Mayadevi, S. *Sep. Sci. Technol.* **1993**, *28*, 2197.
(6) Choudary, V. R.; Mayadevi, S. *Zeolites* **1996**, *17*, 501.
(7) Stach, H.; Lohse, U.; Thamm, H.; Schirmer, W. *Zeolites* **1986**, *6*, 74.
(8) Pascual, P.; Pernot, P.; Ungerer, P.; Tavitian, B.; Boutin, A. *Phys. Chem. Chem. Phys.* **2003**, *5*, 3684.
(9) Ungerer, P.; Beauvais, C.; Delhommelle, J.; Boutin, A.; Rousseau, B.; Fuchs, A. H. *J. Chem. Phys* **2000**, *112*, 5499.
(10) Bourasseau, E.; Haboudou, M.; Boutin, A.; Fuchs, A. H.; Ungerer, P. *J. Chem. Phys.* **2003**, *118*, 3020.
(11) Smit, B. *J. Phys. Chem.* **1995**, *99*, 5597.
(12) Vlugt, T. J. H.; Krishna, R.; Smit, B. *J. Phys. Chem. B* **1999**, *103*, 1102.
(13) Olson, D. H.; Kokotailo, G. T.; Lawton, S. L. *J. Phys. Chem.* **1981**, *85*, 2238.
(14) Bezus, A. G.; Kiselev, A. V.; Lopatkin, A. A.; Du, P. Q. *J. Chem. Soc., Faraday Trans. 2* **1978**, *74*, 367.
(15) Toxvaerd, S. J. *J. Chem. Phys.* **1990**, *93*, 4290.
(16) Toxvaerd, S. J. *J. Chem. Phys.* **1997**, *107*, 5197.
(17) Frenkel, D.; Smit, B. *Understanding Molecular Simulations. From Algorithms to Applications*; Academic Press: New York, 1996.
(18) Marantzas, V. G.; Theodorou, D. N. *Macromolecules* **1998**, *31*, 6310.
(19) Vacatello, M.; Avitabile, G.; Corradini, P.; Tuzi, A. *J. Chem. Phys.* **1980**, *73*, 548.
(20) Smit, B.; Karaborni, S.; Siepmann, J. I. *J. Chem. Phys.* **1995**, *102*, 2126.
(21) Nicholson, D.; Parsonage, N. G. *Computer Simulation and Statistical Mechanics of Adsorption*; Academic Press: New York, 1982.
(22) Ruthven, D. M. *Principles of Adsorption and Adsorption Processes*; Wiley: New York, 1984.
(23) Smit, B.; Maesen, T. L. *Nature* **1995**, *374*, 42.
(24) Zhu, W.; Graaf, J. M.; Broeke, L. J. P.; Kapteijn, F.; Moulijn, J. A. *Ind. Eng. Chem. Res.* **1998**, *37*, 1934.
(25) Maginn, E. J.; Bell, A. T.; Theodorou, D. N. *J. Phys. Chem.* **1995**, *99*, 2057.
(26) Schenk, M.; Vidal, S. L.; Vlugt, T. J. H.; Smit, B.; Krishna, R. *Langmuir* **2001**, *17*, 1558.
(27) Calero, S.; Smit, B.; Krishna, R. *Phys. Chem. Chem. Phys.* **2001**, *3*, 4390.
(28) Krishna, R.; Calero, S.; Smit, B. *Chem. Eng. J.* **2002**, *88*, 81.
(29) Zhu, W.; Kapteijn, F.; Moulijn, J. A.; den Exter, M. C.; Jansen, J. C. *Langmuir* **2000**, *16*, 3322.
(30) Talu, O.; Myers, A. L. *AIChE J.* **2001**, *47*, 1160.